

# Carborane radical anions: spectroscopic and electronic properties of a carborane radical anion with a $2n + 3$ skeletal electron count†

Mark A. Fox,\*<sup>a</sup> Carlo Nervi,<sup>b</sup> Antonella Crivello<sup>b</sup> and Paul J. Low\*<sup>a</sup>

Received (in Cambridge, UK) 4th January 2007, Accepted 20th February 2007

First published as an Advance Article on the web 9th March 2007

DOI: 10.1039/b700110j

One-electron reduction of the well-known carborane 1,2-Ph<sub>2</sub>-1,2-C<sub>2</sub>B<sub>10</sub>H<sub>10</sub> (**1**) gives rise to a stable carborane radical anion ([**1**]<sup>•−</sup>) with a true  $2n + 3$  cluster electron count; the geometry of ([**1**]<sup>•−</sup>) features an elongated C⋯C cage distance but no significant  $\pi$ -bonding interactions between the cage and the phenyl substituents.

The relationships between the composition, number of skeletal electrons and shape of borane-type main-group clusters are familiar topics in inorganic textbooks. Boranes and carboranes adopt closed cage pseudo-spherical deltahedral shapes when there are  $n$  atoms held together by  $2n$  (*hypercloso*) or  $(2n + 2)$  (*closo*) skeletal electrons, whereas progressively more open cluster geometries are associated with clusters offering  $(2n + 4)$  (*nido*),  $(2n + 6)$  (*arachno*) and  $(2n + 8)$  (*hypho*) skeletal electrons.<sup>1</sup> Species with intervening numbers of electrons, *e.g.* radicals with  $(2n + 1)$ ,  $(2n + 3)$  or  $(2n + 5)$  skeletal electrons might be expected to have intermediate shapes to accommodate the unpaired electron.

Radical species with  $n$  skeletal atoms held together by  $(2n + 1)$  skeletal electrons are already known.<sup>2–4</sup> These are *closo* systems lacking one electron, and have the expected closed shapes and connectivities but with slightly expanded bond distances because one bonding MO contains only one electron. The geometries of borane and carborane clusters containing  $2n + 3$  skeletal electrons are intriguing as whilst they occupy the gap between the well-established and abundant closed  $2n + 2$  (*closo*) and open  $2n + 4$  (*nido*) systems little is known about these “missing link” species.<sup>5–8</sup>

Here we report the observation (IR, UV-Vis, ESR) of a stable carborane cluster radical anion derived from the well-known C,C-disubstituted diphenyl-*ortho*-carborane 1,2-Ph<sub>2</sub>-1,2-C<sub>2</sub>B<sub>10</sub>H<sub>10</sub> (**1**). The geometry of this anion has been determined by *ab initio* computations in conjunction with the available experimental data and represents the first clear structural evidence of a stable carborane radical with  $(2n + 3)$  skeletal electrons.

The cyclic voltammogram of **1** in MeCN–0.1 M NBu<sub>4</sub>PF<sub>6</sub> revealed two sequential chemically reversible and electrochemically

quasi-reversible one-electron reduction waves. Successful simulation of the voltammogram was achieved assuming a simple EE mechanism.<sup>9</sup> The *ca.* 170 mV separation of  $E_1$  and  $E_2$  is consistent with a previous report,<sup>7</sup> and gives a measure of the stability of [**1**]<sup>•−</sup> with respect to disproportionation to **1** and [**1**]<sup>2−</sup> ( $K_c = 750$ ) under these conditions. The radical anion [**1**]<sup>•−</sup> was therefore targeted for observation using IR, UV-Vis-NIR and ESR spectroelectrochemical methods.

Reduction of an MeCN–0.1 M NBu<sub>4</sub>BF<sub>4</sub> solution of **1** to [**1**]<sup>•−</sup> caused a shift in the three characteristic  $\nu(\text{BH})$  bands at 2650, 2600 and 2580 cm<sup>−1</sup> to a strong band centred at 2540 cm<sup>−1</sup> (Fig. 1).<sup>10</sup> Further reduction to the dianion [**1**]<sup>2−</sup> was also achieved, with a further shift in the  $\nu(\text{BH})$  band to 2450 cm<sup>−1</sup>. Each progression (**1** to [**1**]<sup>•−</sup> and [**1**]<sup>•−</sup> to [**1**]<sup>2−</sup>) was marked by the development of strict isosbestic points, and the high chemical stability of each redox product was established by the almost complete recovery of the starting spectrum after back-oxidation.

The UV-Vis-NIR spectrum of colourless **1** is characterised by a relatively intense absorption band centred at 44 000 cm<sup>−1</sup> ( $\epsilon$  20 000 M<sup>−1</sup> cm<sup>−1</sup>) (Fig. 2). Reduction to [**1**]<sup>•−</sup> resulted in a dramatic change in the spectroscopic profile, with distinct bands at 20 100, 21 700, 27 500, 28 600 and 31 300 cm<sup>−1</sup> being observed. Further reduction gives a rather broad set of bands between 24 000 cm<sup>−1</sup> and 35 000 cm<sup>−1</sup> for the dianion [**1**]<sup>2−</sup> (Fig. 2). Again, the observation of isosbestic points during the conversion of **1** to [**1**]<sup>•−</sup> and [**1**]<sup>•−</sup> to [**1**]<sup>2−</sup> and the recovery of the original spectra after back-oxidation confirm the chemical reversibility of the redox cycle.

The ESR spectrum of [**1**]<sup>•−</sup>, obtained following electrochemical generation of [**1**]<sup>•−</sup> in an MeCN–0.1 M NBu<sub>4</sub>PF<sub>6</sub> solution, in the ESR cavity gave a broad simple signal confirming its paramagnetic character.† The lack of fine structure in the signal suggests that the unpaired electron is located within the cage, and not localised on

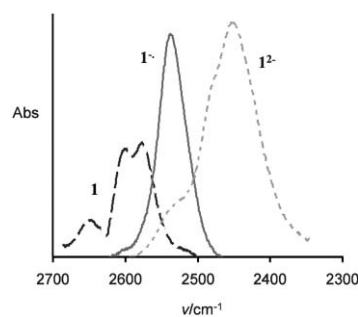
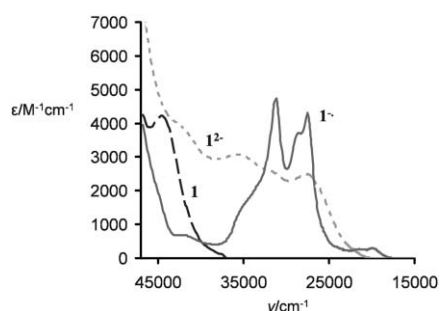


Fig. 1 The IR spectra of **1**, [**1**]<sup>•−</sup> and [**1**]<sup>2−</sup> collected in an OTTLE cell (MeCN, 0.1 M NBu<sub>4</sub>BF<sub>4</sub>).

<sup>a</sup>Department of Chemistry, Durham University, South Rd, Durham, UK DH1 3LE. E-mail: p.j.low@durham.ac.uk; m.a.fox@durham.ac.uk; Fax: +44 191 384 4737; Tel: +44 191 334 2114

<sup>b</sup>Department of Chemistry IFM, University of Torino, via P. Giuria 7, 10125 Torino, Italy

† Electronic supplementary information (ESI) available: Cage numbering schemes, observed and simulated cyclic voltammograms and derived parameters from **1**, together with representative electrochemical data from a selection of other diaryl-*ortho*-carboranes, computational details including Cartesian coordinates of optimised geometries of **1** and [**1**]<sup>•−</sup>, the ESR spectrum of [**1**]<sup>•−</sup>, simulated IR spectra of **1** and [**1**]<sup>•−</sup>, simulated UV spectrum of [**1**]<sup>•−</sup>, and NMR data for **1** and [**1**]<sup>2−</sup>. See DOI: 10.1039/b700110j



**Fig. 2** The UV-Vis spectra of **1**,  $[1]^{-\bullet}$  and  $[1]^{2-}$  collected in an OTTLE cell (MeCN, 0.1 M  $\text{NBu}_4\text{BF}_4$ ).

the phenyl groups.<sup>5</sup> The other members of the series, **1** and  $[1]^{2-}$  (generated by K or Na metal reduction of **1**), were ESR silent and their proton, boron and carbon NMR spectra reveal peaks characteristic of carboranes.<sup>†</sup>

The experimental observations (cyclic voltammetry, IR, UV-Vis-NIR, NMR and ESR spectroscopies) indicate that the *closo*-carborane cluster **1**, which has a  $2n + 2$  cluster electron count, undergoes two sequential one electron reduction processes *via* an EE mechanism to give stable products  $[1]^{-\bullet}$  and  $[1]^{2-}$ , which have  $2n + 3$  and  $2n + 4$  (*nido*) skeletal electron counts respectively. We were able to isolate  $[1]^{-\bullet}$  by chemical reduction with potassium metal in THF. IR, UV and ESR spectra for the isolated salt were identical to those obtained for  $[1]^{-\bullet}$  using the spectroelectrochemical methods described here.

As we have not yet succeeded in obtaining suitable crystals of a  $[1]^{-\bullet}$  salt for crystallographic analysis, we turned to DFT computations (B3LYP/6-31G\*) to link the spectroscopic data obtained from  $[1]^{-\bullet}$  with the underlying molecular and electronic structure. In the interests of maintaining internal consistency in comparisons of **1** and  $[1]^{-\bullet}$ , and as a check of the computational methods employed, compound **1**, which has been structurally characterised by X-ray crystallography,<sup>11</sup> was also examined at the same level of theory.

Infrared spectra were simulated from frequency computations on the optimised geometries for **1** and  $[1]^{-\bullet}$  using Lorentzian curves. The simulation contains three BH bands for **1** near  $2650\text{ cm}^{-1}$ , with a single, somewhat more intense band for  $[1]^{-\bullet}$  at  $2580\text{ cm}^{-1}$ . These calculated vibrational spectra are in excellent agreement with observed data.

Between the optimised geometries of **1** and the radical anion  $[1]^{-\bullet}$ , the most notable structural change is the lengthening of the cage carbon–cage carbon (C1–C2) bond on reduction (Fig. 3). The

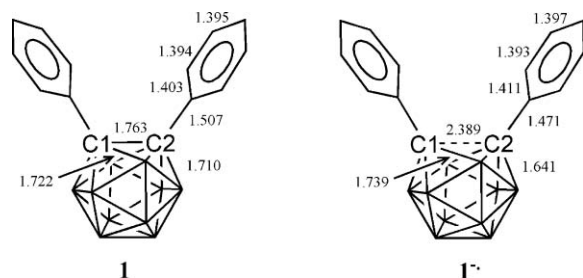


**Fig. 3** Selected bond lengths in the DFT-optimised geometries of **1** and  $[1]^{-\bullet}$ . Each naked vertex of the cages represents BH.

C1–C2 bond lengths for **1** and  $[1]^{-\bullet}$  are 1.76 and 2.39 Å, respectively. Natural bond order (NBO) calculations reveal Wiberg bond orders of 0.59 and 0.06 for the C1–C2 bond in **1** and  $[1]^{-\bullet}$ , respectively. The C1–B4,5 and C2–B7,11 bonds (**1** 1.71 Å;  $[1]^{-\bullet}$  1.64 Å) also contract on reduction. The calculated B3···B6 separation in  $[1]^{-\bullet}$  (2.44 Å), together with the elongated C1–C2 bond (2.39 Å), gives rise to a near square C1–B3–C2–B6 face. Similar diamond–square face relationships are also observed in some diphenylmetallacarboranes.<sup>12</sup>

The phenyl groups are essentially unchanged upon reduction. In diamagnetic carborane anions,  $[1\text{-X-2-Ph-1,2-C}_2\text{B}_{10}\text{H}_{10}]^{-}$ , where an *exo*- $\pi$  double bond exists between the cage carbon and the substituent X<sup>-</sup>, the cage geometries also display elongated C···C intracage bond lengths similar to that calculated here for  $[1]^{-\bullet}$ , accompanied by a contraction of the cage–substituent bonds.<sup>13</sup> However, the  $\text{C}_{\text{cage}}\text{-C}_{\text{ipso}}$  bond lengths in the optimised geometries of **1** and  $[1]^{-\bullet}$  are similar, ruling out such *exo*- $\pi$  bonding character in  $[1]^{-\bullet}$ . Indeed, NBO calculations show Wiberg bond orders of 1.00 and 1.05 for the  $\text{C}_{\text{cage}}\text{-C}_{\text{ipso}}$  bonds in **1** and  $[1]^{-\bullet}$  respectively. The dramatic elongation of the cage C–C bond indicates substantial involvement of the cage in accommodating the additional electron. Computed natural population analysis (NPA) total charges for the cage in **1** and  $[1]^{-\bullet}$  are  $-0.23$  and  $-0.88$ . This increase in negative charge within the cage of  $-0.65$  following reduction of **1** to  $[1]^{-\bullet}$  may be compared with the increase of only  $-0.18$  at each phenyl group. The spectroscopic and computational data all point towards a description of  $[1]^{-\bullet}$  in terms of a chemically stable carborane radical anion with a genuine  $2n + 3$  cluster electron count and *not* an aryl radical anion or an *exo*- $\pi$  type anion.

The frontier orbitals of **1** are largely centred on the phenyl rings, with the large HOMO–LUMO gap (5.78 eV) accounting in part for the stability of this compound (Fig. 4). Time-dependent DFT (TD-DFT) calculations were performed on the optimised geometries of **1** and  $[1]^{-\bullet}$  and the resulting simulated electronic spectra are in excellent agreement with those observed.<sup>†</sup> The high-energy absorption band observed in **1** (Fig. 2) may be attributed to transitions from the three highest occupied orbitals (HOMO, HOMO-1, HOMO-2) to the LUMO, and approximate to  $\pi\text{-}\pi^*$  transitions localised on the phenyl rings (Fig. 4).

Molecular orbital calculations on the optimised geometry for  $[1]^{-\bullet}$  reveal that the compositions of the frontier orbitals

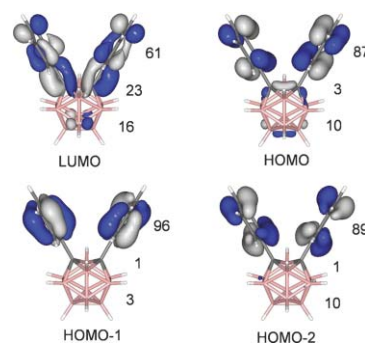


**Fig. 4** Molecular orbitals (B3LYP/6-31G\*) involved in the transitions observed in the UV-Vis spectrum of **1**. The percentage contributions from the phenyl rings, the cage carbon atoms and the other atoms of the cage are given numerically.

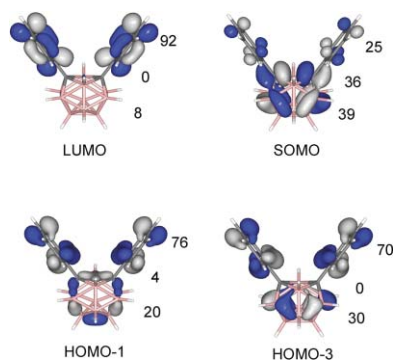


**Fig. 5** Molecular orbitals (B3LYP/6-31G\*) involved in the transitions observed in the UV-Vis spectrum of  $[1]^\bullet-$ . The percentage contributions from the phenyl rings, the cage carbon atoms and the other atoms of the cage are given numerically.

significantly differ from those found in the optimised geometry for **1** (Fig. 5). The SOMO lies 2.74 eV above the next highest occupied orbital (HOMO-1), and the SOMO–LUMO gap is large (3.40 eV). The SOMO is largely associated with the  $C_2B_{10}H_{10}$  cluster core, with some 75% of this orbital being associated with the atoms of the cage. By contrast, the LUMO of **1** has only 39% cage character. The SOMO in  $[1]^\bullet-$  is  $\sigma$  with respect to the C–C vector and is anti-bonding in character. The expansion of the C–C internuclear distance upon reduction of **1** is therefore in keeping with the nodal properties of this orbital.

The TD-DFT computations on the optimised geometry for  $[1]^\bullet-$  successfully reproduce the key features of the electronic spectrum of  $[1]^\bullet-$ , with the lowest energy band of any significant oscillator strength being calculated to fall at  $20\,800\text{ cm}^{-1}$ , and associated largely with the transition from the SOMO to the LUMO. Examination of the compositions of the orbitals involved suggests that this band can be approximated as a cage-to-phenyl ring charge transfer band. Higher energy bands at  $27\,700$  and  $30\,200\text{ cm}^{-1}$  are also calculated and relate well to the observed spectroscopic bands of relatively high intensities near  $28\,600$  and  $31\,300\text{ cm}^{-1}$ . These relatively high energy absorption features correspond to transitions from lower lying fully occupied orbitals (HOMO-1, HOMO-3) with significant phenyl ring character to the cage-centred SOMO.

It is clear that **1** and  $[1]^\bullet-$  are essentially independent species and their frontier orbitals are such that the geometry of  $[1]^\bullet-$  cannot be predicted on the basis of the frontier orbitals of **1**. Similar assumptions may apply to the relationship between  $[1]^\bullet-$  and the little known dianion  $[1]^{2-}$ . Unlike the well-characterised carborane **1**, characterisation of  $[1]^{2-}$  is limited to  $^{13}\text{C}$  NMR data and its geometry has not been determined.<sup>14</sup> Six different geometries are known for 12-vertex carboranes with  $2n + 4$  (*nido*) skeletal electron counts and some are fluxional in solution, pointing to low barriers to interconversion and hinting at the role solvent effects may play in stabilising these species.<sup>15</sup> Further studies of the dianion  $[1]^{2-}$ , including the formation of this species from  $[1]^\bullet-$  by electrochemical and chemical redox methods, are in progress.

In conclusion, one-electron reduction of the well-known 12-vertex cluster 1,2-Ph<sub>2</sub>-1,2- $C_2B_{10}H_{10}$  (**1**) gives rise to a stable carborane radical anion with a true  $2n + 3$  cluster electron count. The addition of an electron above that predicted by electron-counting rules for a *closo*-structure is accommodated by

lengthening of the C–C bond thus generating a near-square face usually associated with open cluster geometries. As hundreds of diaryl-*ortho*-carboranes are known, we expect that carborane radical anions with  $2n + 3$  skeletal electron counts are likely to be a generally accessible family of clusters. Indeed, preliminary studies of a number of substituted diaryl-*ortho*-carboranes reveal similar electrochemical properties to those described here for **1**, which supports this view.

We thank the EPSRC for financial support (MAF, PJJ) and Prof. Ken Wade for discussion of this project. We also thank Prof. Enzo Laurenti for ESR measurements on electrochemically generated samples of **1**.

## Notes and references

- 1 K. Wade, *J. Chem. Soc. D*, 1971, 792; R. E. Williams, *Inorg. Chem.*, 1971, **10**, 210; K. Wade, *Adv. Inorg. Chem. Radiochem.*, 1976, **18**, 1; R. E. Williams, *Adv. Inorg. Chem. Radiochem.*, 1976, **18**, 67; R. E. Williams, *Chem. Rev.*, 1992, **92**, 117.
- 2 W. Einholz, K. Vaas, C. Wieloch, B. Speiser, T. Wizemann, M. Ströbele and H.-J. Meyer, *Z. Anorg. Allg. Chem.*, 2002, **628**, 258; H. Binder, R. Keller, K. Vaas, M. Hein, F. Baumann, M. Wanner, R. Winter, W. Kaim, W. Honle, Y. Grin, U. Wedig, M. Schultheiss, R. K. Kremer, H. G. von Schnering, O. Groeger and G. Engelhardt, *Z. Anorg. Allg. Chem.*, 1999, **625**, 1059; B. Speiser, C. Tittel, W. Einholz and R. Schäfer, *J. Chem. Soc., Dalton Trans.*, 1999, 1741; A. Heinrich, H.-L. Keller and W. Preetz, *Z. Naturforsch., B: Chem. Sci.*, 1990, **45**, 184; V. Lorenzen and W. Preetz, *Z. Naturforsch., B: Chem. Sci.*, 1997, **52**, 565; B. Speiser, T. Wizemann and M. Würde, *Inorg. Chem.*, 2003, **42**, 4018.
- 3 T. Peymann, C. B. Knobler and M. F. Hawthorne, *Chem. Commun.*, 1999, 2039; O. K. Farha, R. L. Julius, M. W. Lee, R. E. Huertas, C. B. Knobler and M. F. Hawthorne, *J. Am. Chem. Soc.*, 2005, **127**, 18243.
- 4 B. T. King, B. C. Noll, A. J. McKinley and J. Michl, *J. Am. Chem. Soc.*, 1996, **118**, 10902; M. J. Ingleson, M. F. Mahon and A. S. Weller, *Chem. Commun.*, 2004, 2398.
- 5 K. A. Bilevich, L. I. Zakharkin and O. Y. Okhlobystin, *Bull. Acad. Sci. USSR, Div. Chem. Sci. (Engl. Transl.)*, 1965, 1887.
- 6 G. D. Mercer, J. Lang, R. Reed and F. R. Scholer, *Inorg. Chem.*, 1975, **14**, 761.
- 7 M. V. Yarosh, T. V. Baranova, V. L. Shirokii, A. A. Érdman and N. A. Maier, *Russ. J. Electrochem.*, 1993, **29**, 1125; M. V. Yarosh, T. V. Baranova, V. L. Shirokii, A. A. Érdman and N. A. Maier, *Russ. J. Electrochem.*, 1994, **30**, 366.
- 8 L. I. Zakharkin, V. N. Kalinin and L. S. Podvisotskaya, *Bull. Acad. Sci. USSR, Div. Chem. Sci. (Engl. Transl.)*, 1967, 2212; L. I. Zakharkin, V. A. Ofshevskaya and B. L. Tumanski, *Metalloorg. Khim.*, 1993, **6**, 98.
- 9 The program ESP (Electrochemical Simulations Package) (C. Nervi) is available free of charge at [http://lem.ch.unito.it/chemistry/esp\\_manual.html](http://lem.ch.unito.it/chemistry/esp_manual.html).
- 10 T. Mahabiersing, H. Luyten, R. Nieuwendam and F. Hartl, *Collect. Czech. Chem. Commun.*, 2003, **68**, 1687; F. Hartl, H. Luyten, H. A. Nieuwenhuis and G. C. Schoemaker, *Appl. Spectrosc.*, 1994, **48**, 1522.
- 11 Z. G. Lewis and A. J. Welch, *Acta Crystallogr., Sect. C: Cryst. Struct. Commun.*, 1993, **C49**, 705.
- 12 A. J. Welch, Steric effects in metallacarboranes, in *Metal Clusters in Chemistry*, ed. P. Braunstein, L. A. Oro and P. R. Raithby, Wiley-VCH, Weinheim, 1999, vol. 1, p. 69.
- 13 D. A. Brown, W. Clegg, H. M. Colquhoun, J. A. Daniels, I. R. Stephenson and K. Wade, *J. Chem. Soc., Chem. Commun.*, 1987, 889; T. D. Getman, C. B. Knobler and M. F. Hawthorne, *J. Am. Chem. Soc.*, 1990, **112**, 4593; K. Chui, H.-W. Li and Z. Xie, *Organometallics*, 2000, **19**, 5447; L. A. Boyd, W. Clegg, R. C. B. Copley, M. G. Davidson, M. A. Fox, T. G. Hibbert, J. A. K. Howard, A. Mackinnon, R. J. Peace and K. Wade, *Dalton Trans.*, 2004, 2786.
- 14 M. A. Fox, Polyhedral carboranes, in *Comprehensive Organometallic Chemistry III*, ed. R. H. Crabtree and D. M. P. Mingos, Elsevier, Oxford, 2007, vol. 3, p. 49.
- 15 L. I. Zakharkin, V. N. Kalinin, V. A. Antonovich and E. G. Rys, *Bull. Acad. Sci. USSR, Div. Chem. Sci. (Engl. Transl.)*, 1976, 1009.